Simulating enhanced ocean alkalinity experiments in a high-latitude fjord using nested ROMS simulations coupled with MARBL biogeochemistry

Supplementary Information

***Ulla K. Heede**[1], Matthew C. Long[1], Alicia Karspeck[1], Scott Bachman[1], Nora Loose[1], Dafydd Stephenson[1], David T. Ho[2], Lennart Gerke[1], Tobias Koffman[2], Alice Benoit-Cattin[3]; Sara Harðardóttir[3], and Andreas Macrander[3]*

[1] *[C]Worthy, Boulder, Colorado, USA*
[2] *Department of Oceanography, University of Hawai'i at Mānoa, Honolulu, Hawaii, USA*
[3] *Marine and Freshwater Research Institute (MFRI), Hafnarfjörður, Iceland*

***Corresponding author:** Ulla K. Heede, 1909 Broadway Ste 200, Boulder, CO 80302, USA, ulla@cworthy.org.*

River dataset

Field data for the Hvalfjörður river dataset was collected on July 25, 2024, between 10:00 and 15:00 under dry conditions with an air temperature of approximately 14 °C and partly sunny skies. A total of 16 rivers were directly measured, limited to sites that were physically accessible (i.e., not fenced and with adequate parking). For each accessible river, width, depth, and flow velocity were measured or estimated. Discharge was calculated assuming a half-elliptical channel cross-section, using the expression: A=(width x depth x π)/2 and multiplying by surface velocity.

Velocity was estimated by timing a floating object over a known distance. In deeper rivers, depth could not always be directly measured and was therefore approximated based on the apparent slope from the riverbank and visual assessment of bottom visibility. Rivers were categorized by discharge as follows: Category 0 (<0.5 $m^3 s^{-1}$), Category 1 (0.5–1 $m^3 s^{-1}$), Category 2 (1–2 $m^3 s^{-1}$), and Category 3 (>2 $m^3 s^{-1}$). All Category 2 and 3 rivers were measured directly. For rivers that were not accessible, satellite imagery was used to estimate their size. These rivers were assigned discharge values based on the average measured discharge within their corresponding flow category.

This data was then formed into a river forcing dataset in roms-tools with monthly average discharge values for each river, with the mouth of the rivers adjusted to the relevant mask. The river discharge was assumed for simplicity to be null during winter months (November through March, where average temperatures were below 0 °C) and about 60% of the measured values during summer months as an initial iteration with 100% of the measured volume showed too much freshwater relative to the observed stratification.

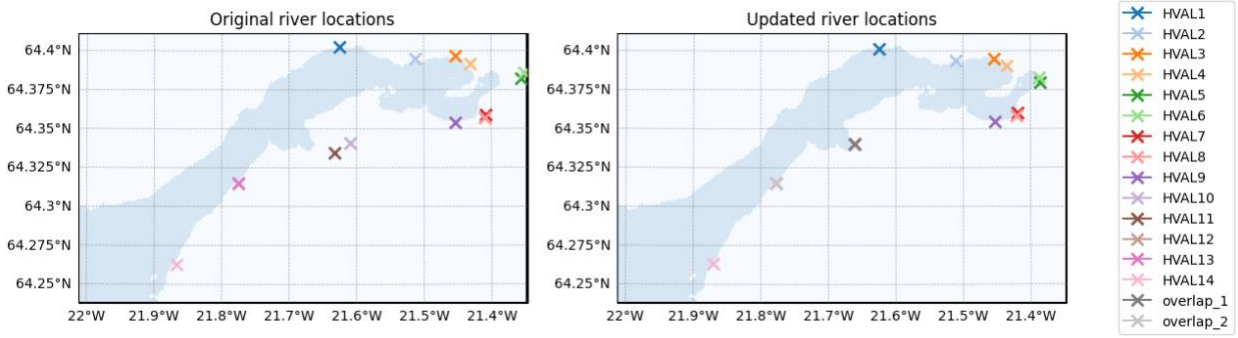

Figure S1. *Overview of river locations from roms-tools dataset generation.*

Scenario	Alk (background) (mmol/m³)	DIC (mmol/m³)	PO_4 (mmol/m³)	Si (mmol/m³)	T (°C)	S(psu)
Model	2320	2110.0	0.8	6.8	11.5	33.75
Obs	2380	2160.0	0.3	2.0	10	33.75

Table S1. *Background values used in CO2SYS to calculate the carbonate chemistry response to an alkalinity addition.*

	pCO2	pH	Alk	DIC
Detectability limit	+/- 9.2 ppvm	Above 8.12 (July) Above 8.15 (November)	+/- 5 mmol/m³ (July) +/- 6 mmol/m³ (Nov)	+/- 26 mmol/m³ (July) +/- 11 mmol/m³ (Nov)

Table S2. Table showing approximate detectability limits in Hvalfjörður *for relevant carbonate chemistry variables. We determined the pCO2 detectability limit by calculating the standard deviation of pCO2 data for the month of November 2024 from a sensor installed at the Pier (see Fig. 1) at depth 0.2 m by the Röst Marine Research Centre. We determined the pH detectability by calculating the average standard deviation of pH variability for the months of July and November 2024 from the pH data at mooring HVIN (Fig. 1). We determined the alkalinity and DIC detectability limits by calculating the average standard deviation of salinity normalized Alkalinity and DIC values taken by samples in July and November 2024 at Sample station 10 (Fig. 1).*

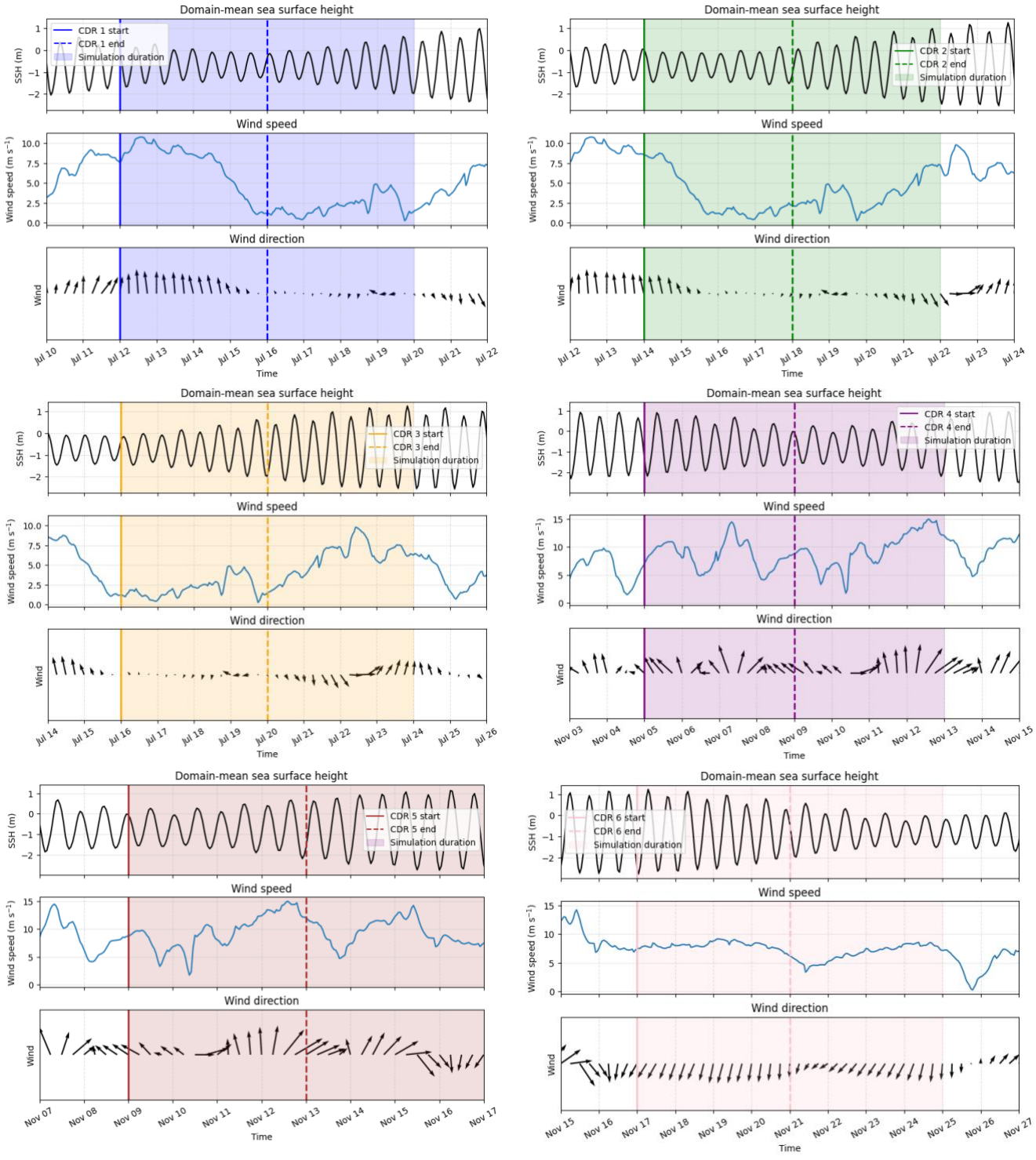

Figure S2. *Wind and tidal conditions for each OAE release.*

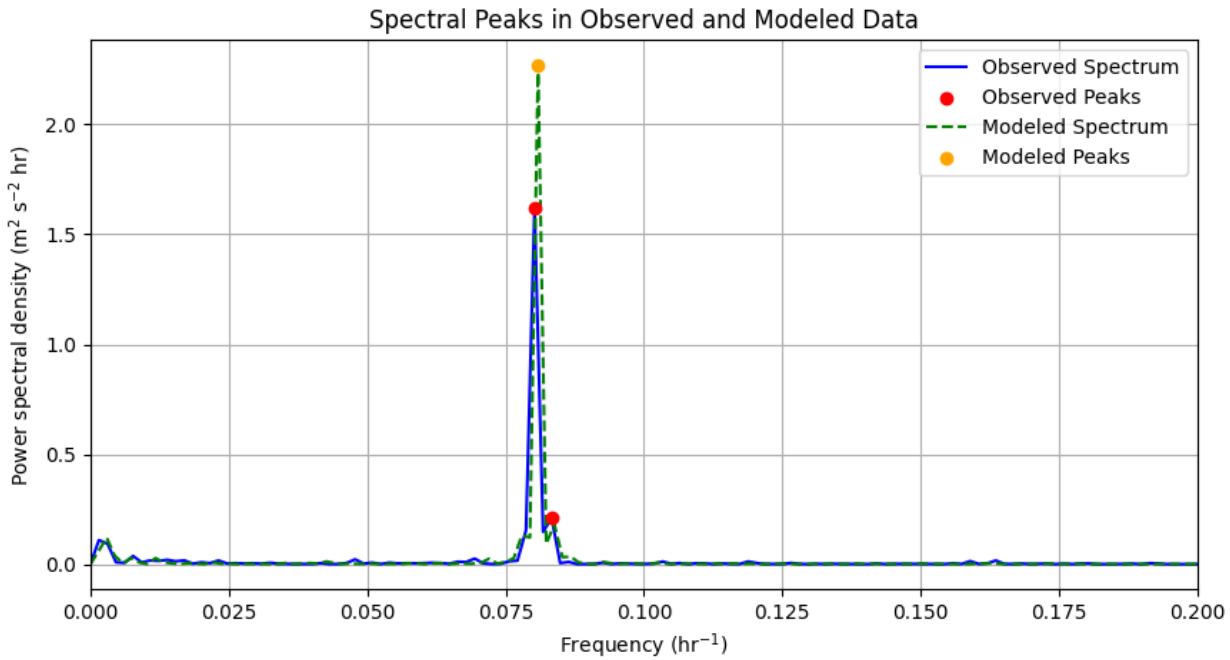

Figure S3. Power spectral density (PSD) of observed and modeled northward velocity at mooring HVNV. *The spectra are computed from 10-minute averaged velocity time series at 10 m depth for the period 5–31 July 2024 using a normalized Fourier transform, yielding PSD in units of m² s⁻² hr. The blue curve shows the observed spectrum and the green dashed curve shows the modeled spectrum; markers indicate dominant spectral peaks identified from each time series.*

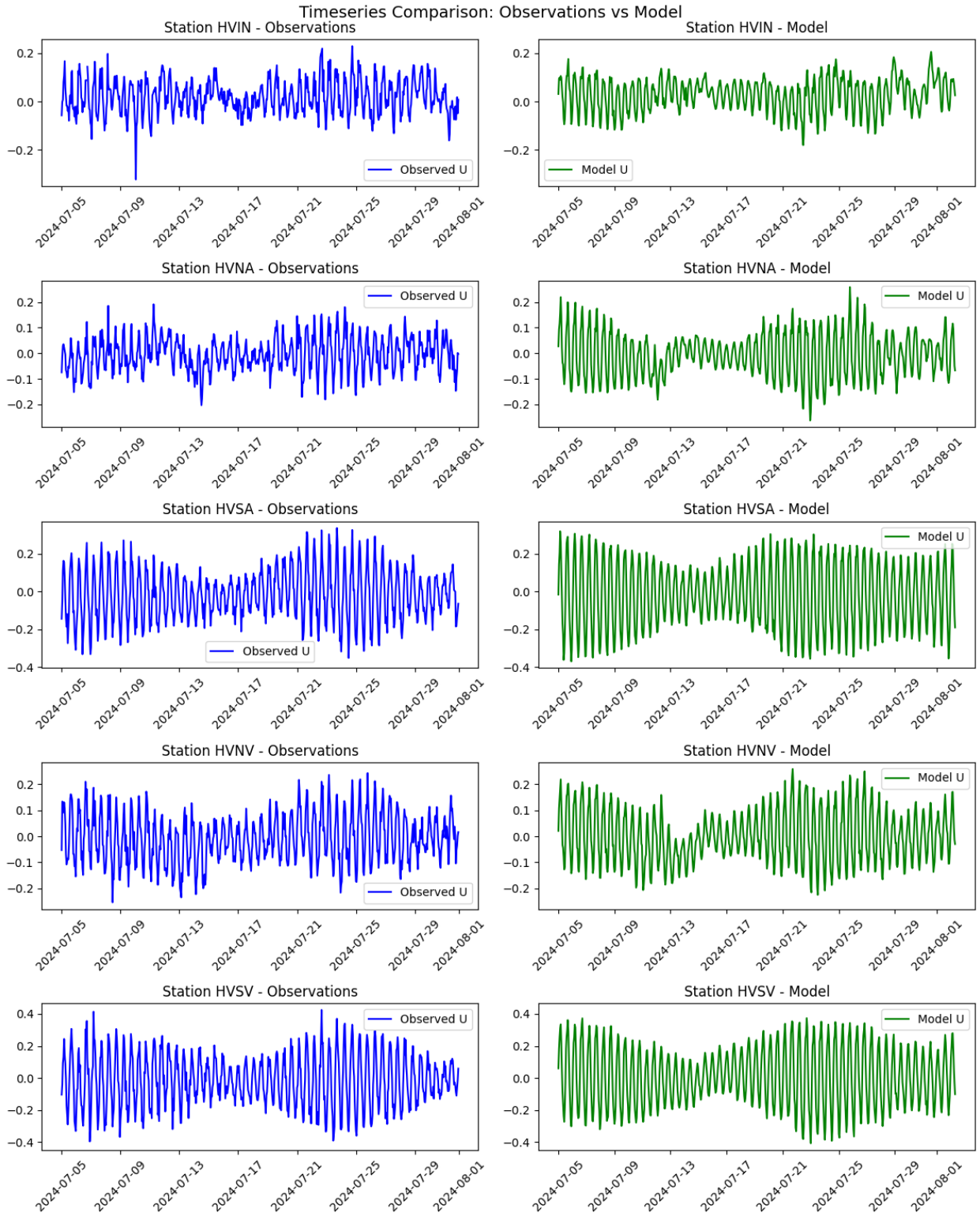

Figure S4. Eastward velocities from the ADCP moorings (left) and model corresponding locations (right) at 10 m depth.

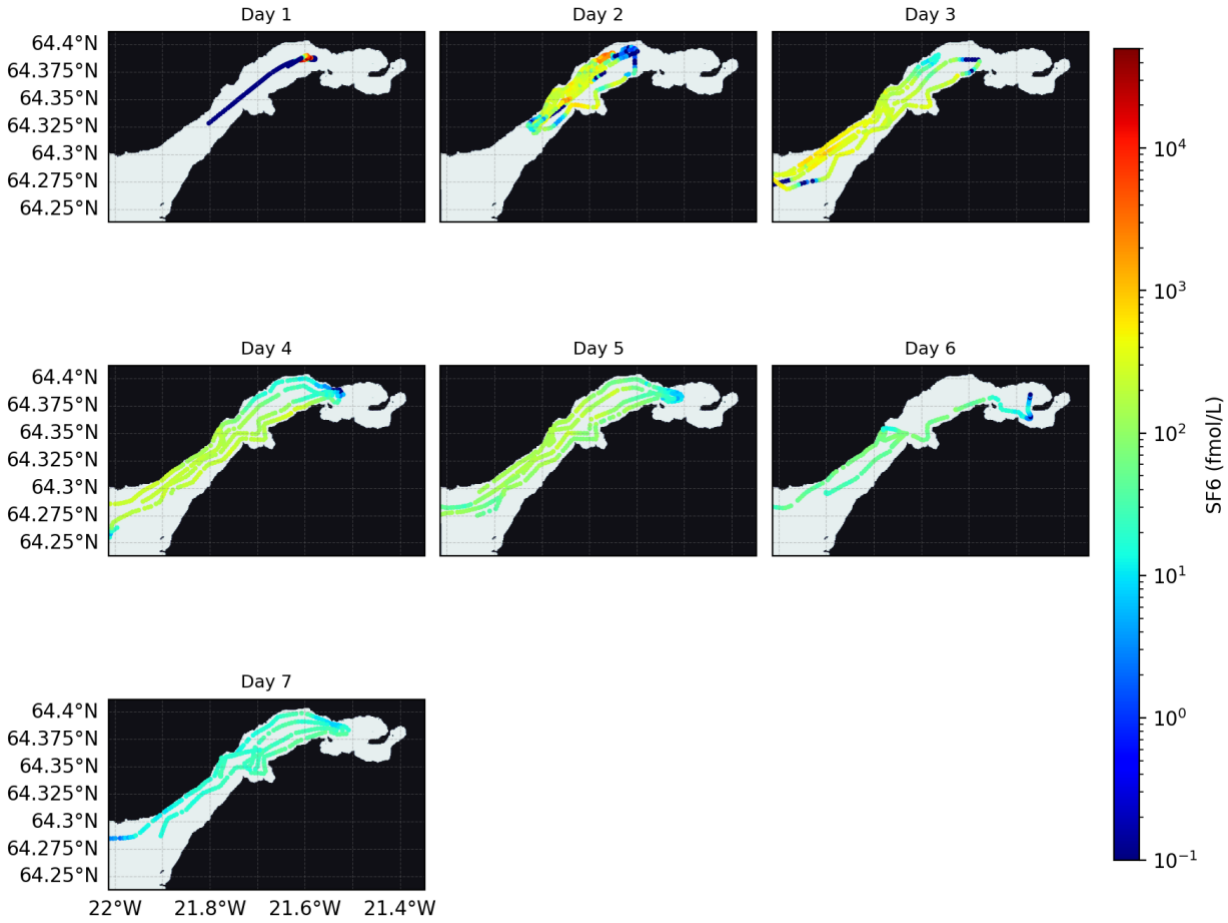

Figure S5. *Locations and measured SF6 values for each day.*

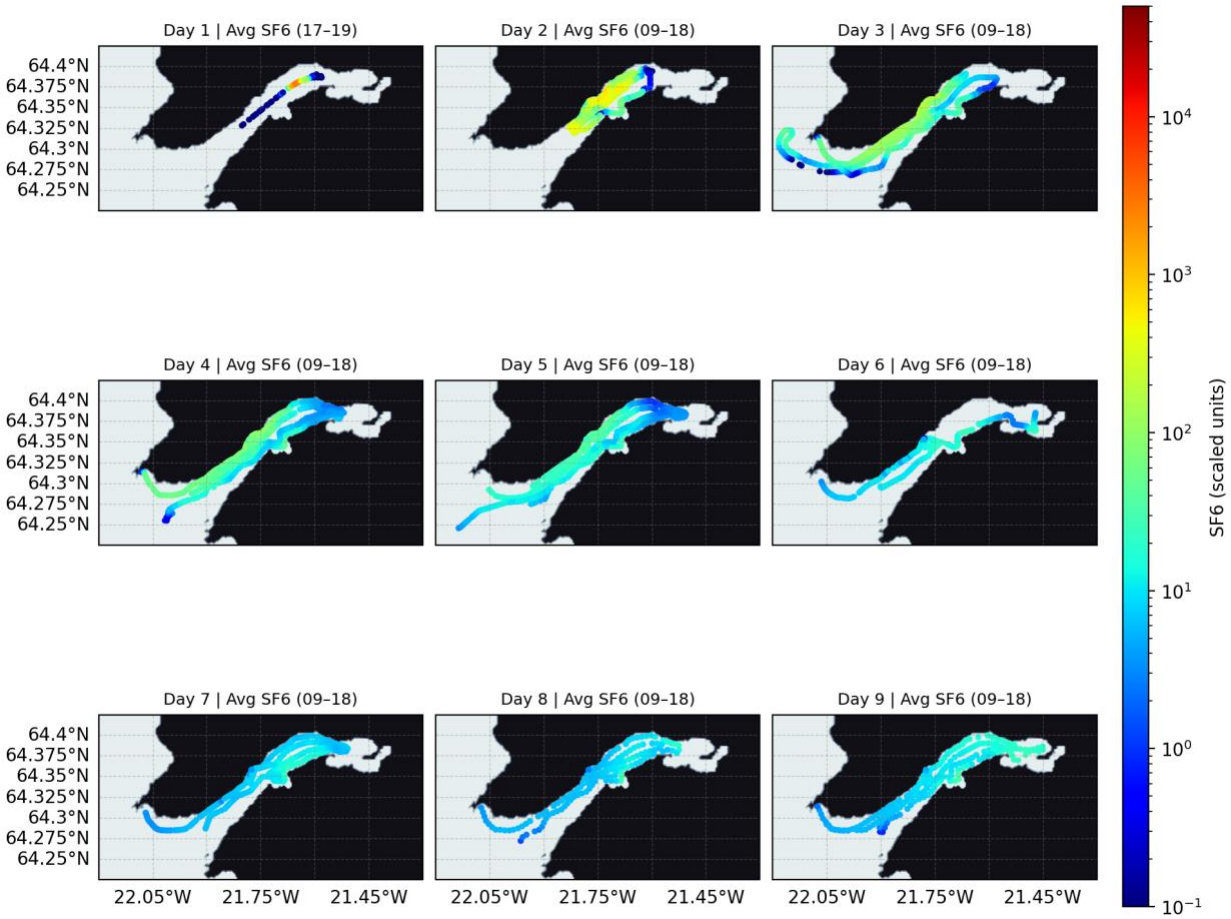

Figure S6. *Locations and modeled SF6 values for each day.*

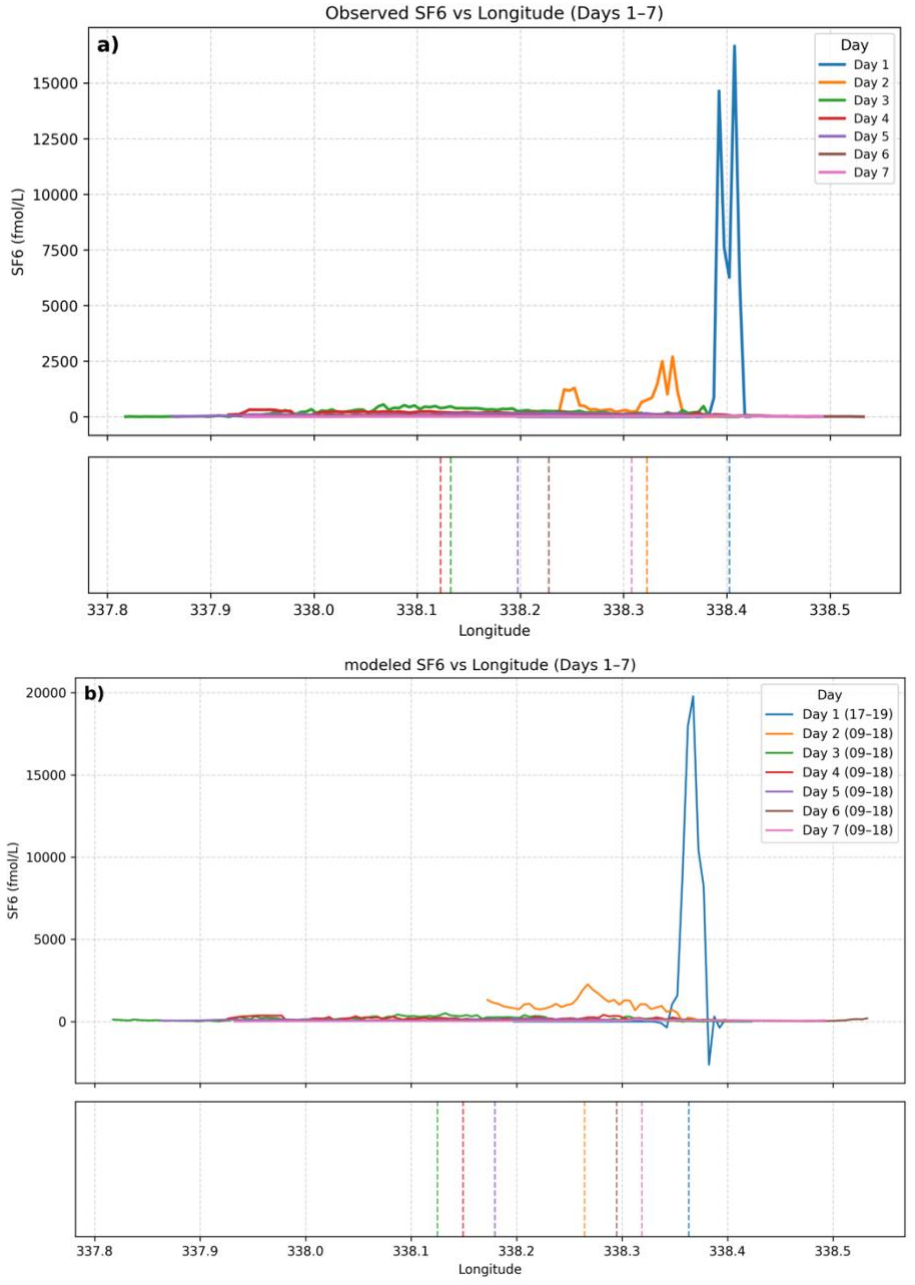

Figure S7. *As Figure 5 but with the scale adjusted to show the values on day 1. Note the negative tracer values in the model are caused by a non-monotonic conservative advection scheme in ROMS, which can cause negative values with sharp spatial gradients, but the total mass of tracer is conserved.*

Figure S8. *Nutrient values at the surface and at depth over the 2024-2025 field season from observations (left) and model (right). Model is sampled at locations and times where observational data exists (note, for the winter months of 2025, the model 2024 data is used).*

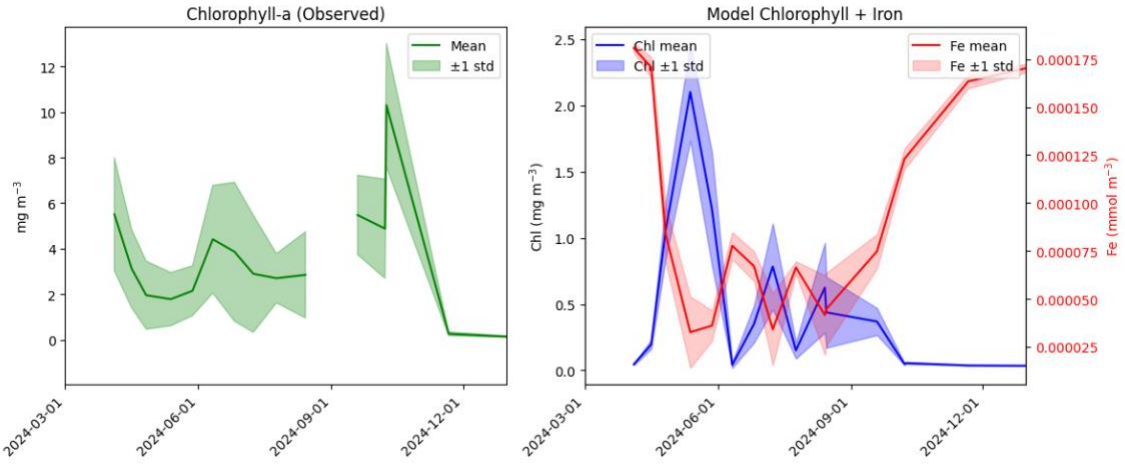

Figure S9. *Observed and model chlorophyll concentrations throughout the 2024-2025 field season, with the modeled chlorophyll concentration shown alongside the iron concentrations.*

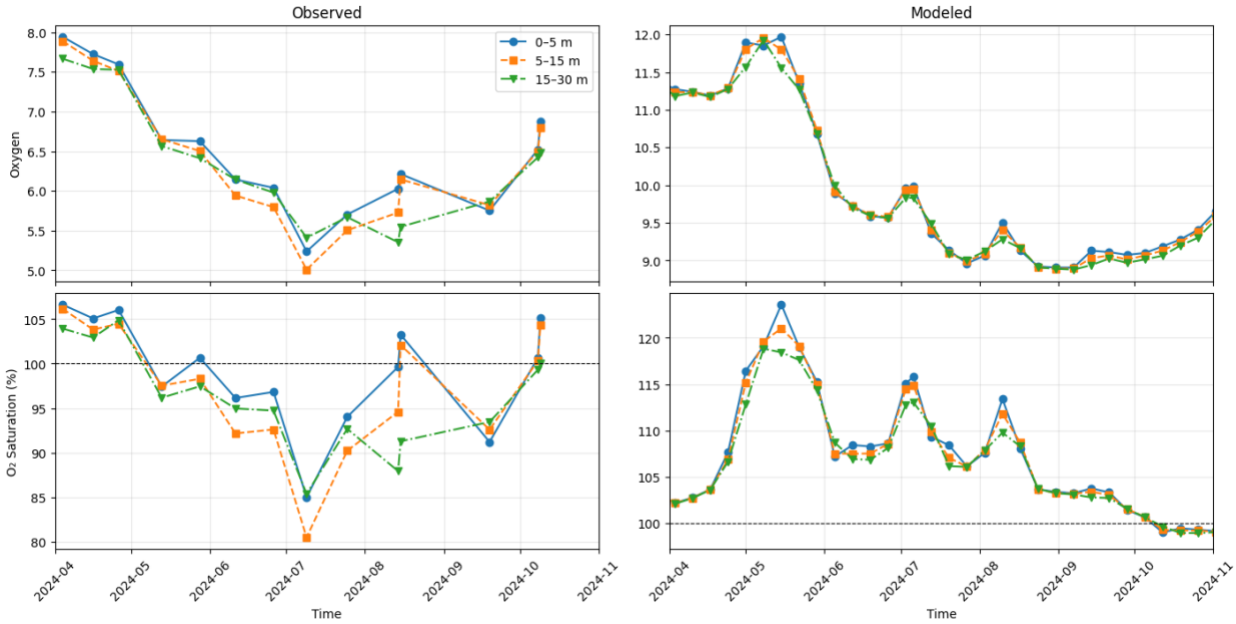

Figure S10. *Time series of oxygen and oxygen saturation in the surface layer, mid-layer and at depth for observations (left) and model (right). Model data is sampled at locations and times where observational data exists. Note that the y-axis is different in the right and left columns.*

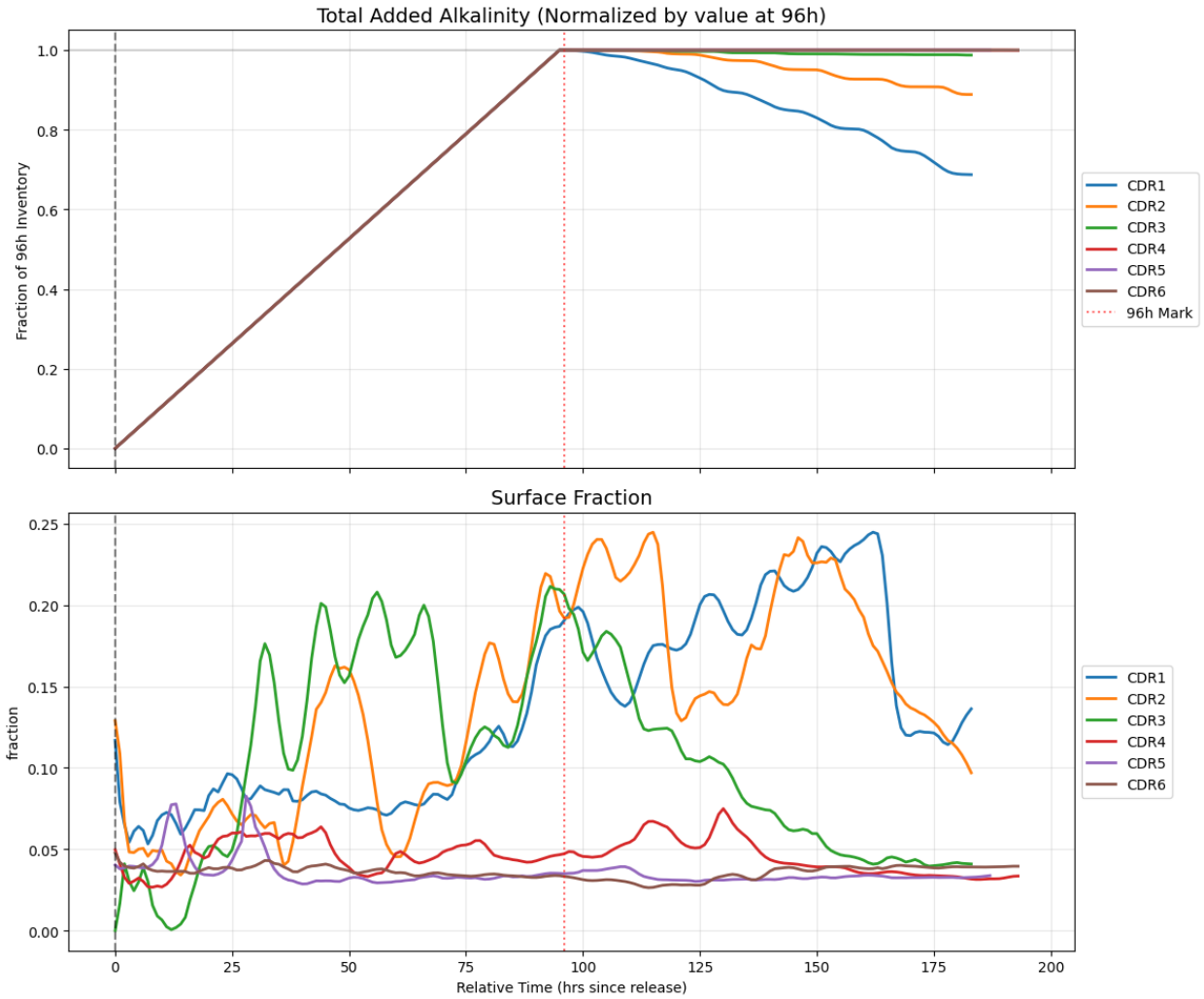

Figure S11. *The upper panel illustrates the added alkalinity in the domain, represented as a fraction of the maximum value. The lower panel depicts the fraction of added alkalinity localized within the surface layers.*

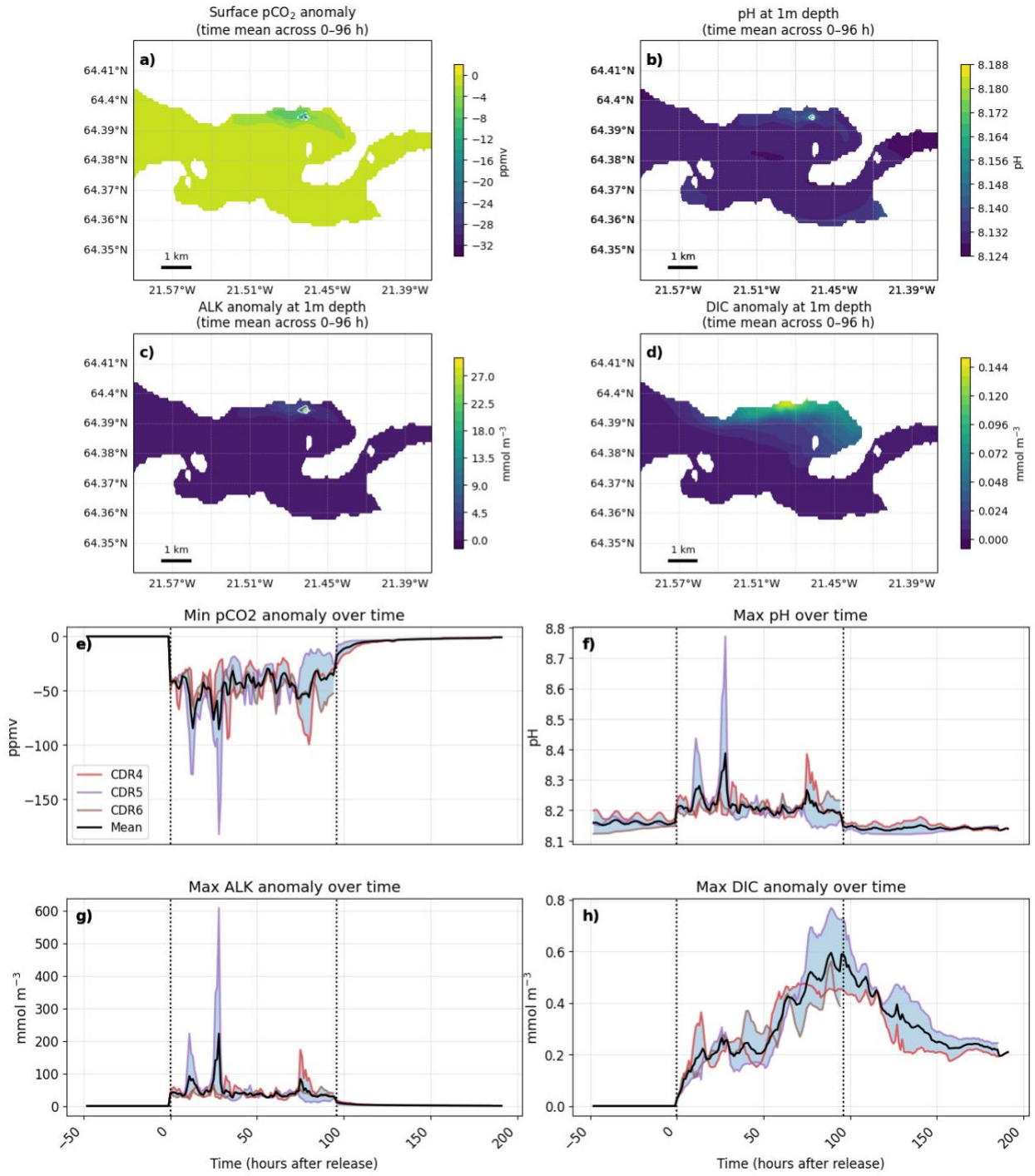

Figure S12. *As Fig. 10 but for the November ensembles (CDR4, CDR5 and CDR6).*